Stiffness-changing of Polymer Nanocomposites with Cellulose Nanocrystals and Polymeric Dispersant

Worarin Meesorn,[1] Justin O. Zoppe[1,2] and Christoph Weder[1,]*

[1]Adolphe Merkle Institute, University of Fribourg, Chemin des Verdiers 4, 1700 Fribourg, Switzerland

[2]Omya International AG, Baslerstrasse 42, CH-4665, Oftringen, Switzerland

*To whom correspondence should be addressed, e-mail: christoph.weder@unifr.ch

Abstract

We report bio-inspired, water-responsive, mechanically adaptive nanocomposites based on cellulose nanocrystals (CNCs), poly(ethylene oxide-*co*-epichlorohydrin) (EO-EPI), and a small amount of poly(vinyl alcohol) (PVA), which was added to aid the dispersion of the CNCs. In the dry state, the CNCs form a reinforcing network within the polymer matrix, and the substantial stiffness increase relative to the neat polymer is thought to be the result of hydrogen-bonding interactions between the nanocrystals. Exposure to water, however, causes a large stiffness reduction, due to competitive hydrogen bonding of water molecules and the CNCs. We show here that the addition of PVA to the EO-EPI/CNC nanocomposite increases the modulus difference between the dry and the wet state by a factor of up to four compared to the nanocomposites without the PVA. The main reason is that the PVA leads to a substantial increase of the stiffness in the dry state; for example, the storage modulus E' increased from 2.7 MPa (neat EO-EPI) to 50 MPa upon introduction of 10% CNCs, and to 200 MPa when additionally 5% of PVA were added. By contrast, the incorporation of PVA only led to moderate increases of the equilibrium water swelling and the E' in the wet state.

Main Text

The groups of Weder and Rowan pioneered the development of a family of polymer nanocomposites that change their mechanical properties upon exposure to water.[1-4] The materials were inspired by the function and operating principle of the skin of sea cucumbers, which displays mechanically adaptive behavior.[5-14] The bio-inspired nanocomposites were comprised of a polymer matrix and rigid, high-aspect ratio cellulose nanocrystals (CNCs). In the dry state, the CNCs form a reinforcing network within the polymer matrix, and the substantial stiffness increase relative to the neat polymer is thought to involve hydrogen-bonding interactions between the nanocrystals. Consequently, when such materials are exposed to water, a large stiffness reduction can be observed, due to competitive hydrogen bonding[15, 16] of the water molecules and the hydroxyl groups present on the surfaces of the CNCs. The first generation of such materials involved a low-modulus ethylene oxide-epichlorohydrin (EO-EPI) copolymer and CNCs isolated from tunicates (for chemical structures, see **Figure 1**). The incorporation of the latter resulted in a 200-fold increase of the dry storage modulus E' from a few MPa (neat EO-EPI) to almost one GPa. The nanocomposites undergo a reversible modulus reduction from up to 800 to 20 MPa upon exposure to water. The effect was in the meantime demonstrated in numerous compositions, which include many other rubbery,[17-19] and also glassy matrix polymers.[20-22] In the latter, water-induced plasticization further increases the modulus difference. The decoration of CNCs with specific binding motifs has also allowed extending the effect to other stimuli.[23-26] Several nanomaterials have been used to create such adaptive nanocomposites,[27-29] but CNCs remained the filler of choice, due to their high strength (0.25-6 GPa)[20, 30] and stiffness (105-150 GPa),[31-33] benign nature, and the renewability and low cost of the sources from which they are isolated.[34, 35] The properties of CNCs depend on the source from which they are extracted and also the isolation

2

process.[36, 37] From a mechanical perspective, CNCs isolated from tunicates with an aspect ratio A of ca. 80 and an on axis elastic modulus E of ca. 150 GPa[33, 38] are preferable over CNCs isolated from wood or cotton pulp (A=11, E=105 GPa). Apart from the intrinsically higher stiffness and strength, high-aspect-ratio CNCs reach the percolation threshold at a lower concentrations than lower-aspect-ratio CNCs.[39, 40] They also aggregate less, on account of kinetic arrest[41] and also because reinforcement can be achieved at a lower filler content. A comparison of nanocomposites of poly(ethylene oxide-*co*-epichlorohydrin) (EO-EPI) and CNCs isolated from either cotton or tunicates shows that at all compositions, the former offer a much less pronounced reinforcement than the latter. Based on the notion that CNCs isolated from tunicates are unlikely to be viable for large-scale applications and that the availability and (projected) costs seem to favor low-aspect ratio CNCs (such as those isolated from cotton or wood pulp), our group recently embarked on investigating possibilities to maximize the reinforcing effect of low-aspect-ratio cotton-derived CNCs. For example, we combined two rod-like particle types with different aspect ratio, and showed that a significant portion of the high-aspect-ratio CNCs can be substituted with low-aspect-ratio CNCs without changing the properties much.[41] We further discovered that adding a small amount of poly(vinyl alcohol) (PVA) can significantly influence the mechanical properties of nano-composites of EO-EPI and CNCs isolated from cotton, on account of better CNC dispersion. Remarkably, when 5% w/w of PVA were added to EO-EPI, the tensile strength and Young's modulus showed a 5-fold increase in comparison to the PVA-free nanocomposites.[42] We show here that this framework can also be exploited to increase the extent by which the stiffness of polymer/CNC nanocomposites can be switched upon exposure to water. Using again EO-EPI/PVA nanocomposites with CNCs isolated from cotton as a testbed, we demonstrate that the ratio of the storage moduli in the dry and the wet state can be increased by a factor of up to four compared to

3

the nanocomposites without the PVA. This is important for some biomedical applications *e.g.* cortical implants, which require materials that are rigid enough to facilitate insertion, but soften thereafter,[43, 44] and with a stiffer nanocomposite, the implant size can be reduced.
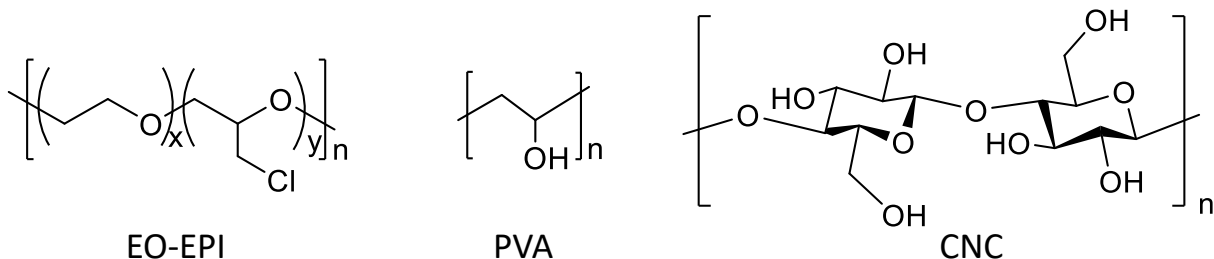

Figure 1. Chemical structures of ethylene oxide-epichlorohydrin (EO-EPI) copolymer, poly(vinyl alcohol) (PVA), and cellulose nanocrystals (CNC).

Two series of EO-EPI/PVA/CNC nanocomposites were prepared according to a previously reported protocol, which involves solvent casting, drying, and subsequent compression molding.[42] In a first series, the CNCs content was kept constant at 10% w/w and the PVA content was varied (1, 3, and 5% w/w); a PVA-free EO-EPI/CNC reference nanocomposite was also prepared. In a second series, the PVA content was kept constant at 5% w/w, and the CNC content was varied (5, 7, 9, 15, and 20% w/w). We first investigated the swelling behavior of all nanocomposites by monitoring the mass increase of thin films upon immersion in water. The data shows that in all cases equilibrium swelling has been reached after 15-20 minutes and that the degree of swelling at equilibrium depends on the amount of PVA and CNC in the nanocomposites (**Figure 2**). **Figure 2a** displays that the equilibrium water uptake is increased from ~3% (neat EO-EPI) to ~11% upon introduction of 10% w/w CNCs. This is qualitatively consistent with previous reports[17, 20-22] (although the water-takeup and water-induced switching of EO-EPI composites with CNCs isolated from cotton has not been investigated) and the previous observation that the hydrophilic

CNCs can adsorb water and act as water transport channels.[18, 19] With the incorporation of only 1% w/w PVA in addition to 10% w/w CNCs, the water uptake further increased to ~14%, but there was no significant change in water uptake when the PVA content was increased to 5% w/w (**Table 1**). This seems to suggest that the water take-up is mainly driven by the CNCs. We further investigated the swelling behavior of EO-EPI/PVA/CNC nanocomposites in which the PVA content was fixed at 5% w/w and the CNC content was varied between 5 and 20% w/w. As expected, the equilibrium water uptake of the nanocomposites increased with the CNC content, *i.e.*, from 4.6% (for EO-EPI/5%PVA/5%CNC) to 19% (for EO-EPI/5%PVA/20%CNC) (**Figure 2b**, **Table 1**). The data suggest that PVA, which as we previously demonstrated is localized on the CNCs' surface and helps to disperse these particles in the EO-EPI matrix,[42] mainly acts by preventing CNC aggregation and thereby helping to form a water-transporting CNC network. On the other hand, the small amounts of PVA introduced in the materials studied, only caused a small enhancement of the water uptake of EO-EPI/PVA/CNC nanocomposites.

In order to explore if the PVA might be dissolved and released from the nanocomposite upon immersion in water, we functionalized the PVA with fluorescein (PVA-F), which shows green fluorescence upon exposure with UV light and can be utilized to monitor PVA leaching. EO-EPI/PVA-F/CNC nanocomposite films containing 10% w/w CNCs and 5% w/w fluorescein-labelled PVA-F were prepared by casting from DMSO. The green fluorescence emitted by the dried film can readily be seen under UV light (**Supporting Figure S1a**). While a reference solution containing 50 µg/mL fluorescein-labelled PVA-F in water (a concentration that corresponds to the value achievable if PVA-F extraction during immersion in water was quantitative) also shows green fluorescence under UV light, whereas the water in which the EO-EPI/PVA-F/CNC nanocomposite film had been immersed for 24 h showed no detectable fluorescence (**Supporting**

Figure S1b). The absorption and emission spectra of PVA-F solution and nanocomposite immersed water (**Supporting Figure S2**) also confirm that the extraction of PVA from the nanocomposites does not occur, at least not within a timeframe of a day.

(a) (b)
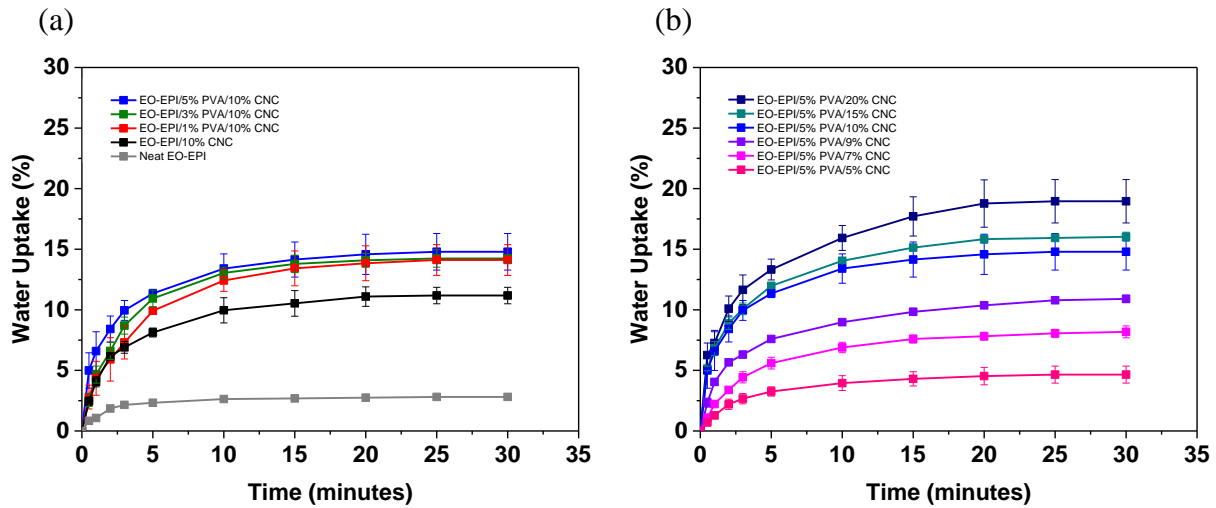
Figure 2. Water uptake as a function of immersion time of (a) neat EO-EPI and EO-EPI/PVA/CNC nanocomposites containing 10% w/w CNCs and 0-5% w/w PVA; and (b) EO-EPI/PVA/CNC nano-composites containing 5% w/w PVA and 5-20% w/w CNCs. Data were acquired at ambient temperature.

(a) (b)
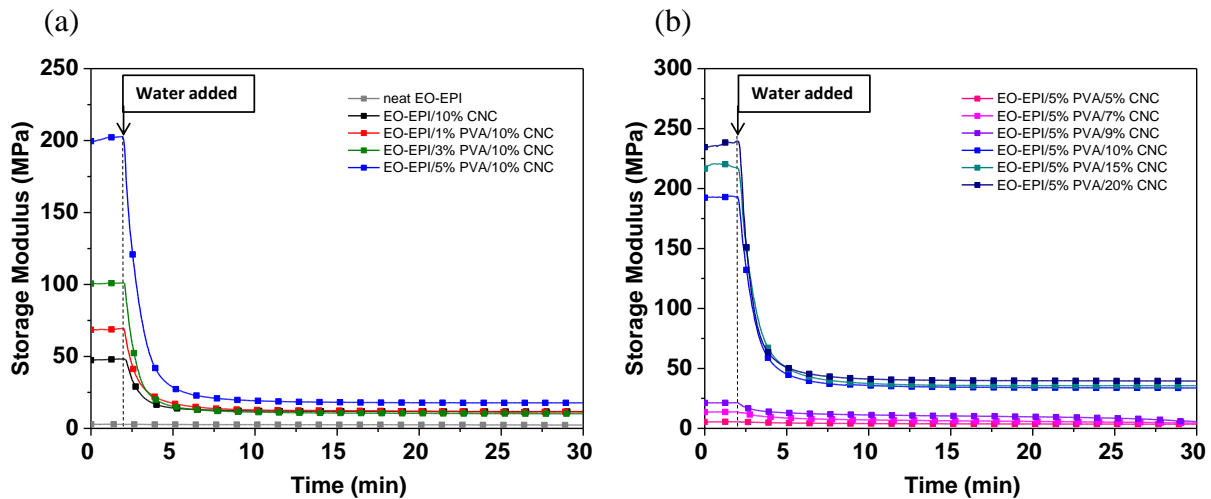
Figure 3. Storage moduli as a function of time, documenting the mechanical switching of (a) neat EO-EPI and EO-EPI/PVA/CNC nanocomposites containing 10% w/w CNCs and 0-5% w/w PVA;

6

and (b) EO-EPI/PVA/CNC nanocomposites containing 5% w/w PVA and 5-20% w/w CNCs upon immersion into water at the time indicated. Data were acquired at ambient temperature.

Table 1. Storage moduli of dry and water-swollen EO-EPI/PVA/CNC nanocomposites and their water uptake at equilibrium.

Composition	Storage Modulus[a], E' (MPa)		Modulus difference,[b] $\Delta E'$ (MPa)	Water uptake at equilibrium[c] (%)
	dry state	wet state		
Neat EO-EPI	2.7 ± 0.03	2.1 ± 0.01	0.6 ± 0.04	2.9 ± 0.1
EO-EPI/10%CNC	50 ± 6	11 ± 1	39 ± 7	11.2 ± 0.7
EO-EPI/1%PVA/10%CNC	68 ± 2	11 ± 1	57 ± 3	14.1 ± 1.3
EO-EPI/3%PVA/10%CNC	107 ± 8	11 ± 1	96 ± 9	14.2 ± 0.3
EO-EPI/5%PVA/10%CNC	200 ± 6	30 ± 11	170 ± 17	14.8 ± 1.5
EO-EPI/5%PVA/5%CNC	5.0 ± 0.8	3.3 ± 0.3	1.7 ± 1.1	4.6 ± 0.7
EO-EPI/5%PVA/7%CNC	14.2 ± 0.3	6.1 ± 2.8	8.1 ± 3.1	8.2 ± 0.5
EO-EPI/5%PVA/9%CNC	20.7 ± 0.8	7.1 ± 1.5	13.6 ± 2.3	10.9 ± 0.3
EO-EPI/5%PVA/15%CNC	216 ± 1	33 ± 4	183 ± 5	16.0 ± 0.4
EO-EPI/5%PVA/20%CNC	246 ± 23	34 ± 9	202 ± 32	19.0 ± 1.8

[a]Data were acquired from DMA analyses at ambient temperature and represent averages of $N = 3$ individual measurements ± standard deviation. [b]Between the dry and the wet state. [c]Data were acquired from weight measurements of nanocomposites films that had been immersed in water at ambient temperature for 30 min and represent averages of $N = 3$ individual measurement ± standard deviation.

We next investigated the mechanical properties of the EO-EPI/PVA/CNC (and EO-EPI/CNC) nanocomposites in the dry state and after immersion in water with dynamic mechanical analysis (DMA) at ambient temperature. The experiments were conducted in a setup that allowed monitoring the mechanical switching, i.e., the change of the storage modulus E' upon exposure to water as a function of time. In the dry state, the storage modulus, E' of the nanocomposites films was increased upon increasing of CNCs and PVA content, i.e., the addition of 10-20% w/w CNCs

(above the percolation threshold) with 1-5% w/w PVA has a very significant impact on the mechanical properties of the nanocomposites as reported in our previous study.[42] For example, E' at ambient temperature increased from 2.7 ± 0.03 MPa for the neat polymer to 50 ± 6 MPa for the nanocomposite with 10% w/w CNCs, and further increased to 200 ± 6 MPa when in addition to 10% w/w CNCs 5% w/w PVA were added. E' increased further when the PVA content was kept ix at 5% w/w and the CNC content was increased to 15% ($E' = 216 ± 1$ MPa) or 20% w/w CNCs ($E' = 246 ± 23$ MPa) (**Figure 3, Table 1**). Upon immersion in water, the neat EO-EPI film does not show a significant change in mechanical properties, while a drastic drop in E' was observed in all of the nanocomposites. For instance, the EO-EPI/10%CNC nanocomposite shows an E' of 50 ± 6 MPa in the dry state and an E' of 11 ± 1 MPa in the water-swollen state, which corresponds to a difference of 39 ± 7 MPa, or a reduction by a factor of 4.5. The EO-EPI/5%PVA/10%CNC displays an E' of 200 ± 6 MPa in the dry state, which drops to 30 ± 11 MPa in the wet state, i.e., the difference corresponds to 170 ± 17 MPa (a four-fold increase over the PVA-free material) or a reduction by a factor of 6.7. The modulus difference further increased with the CNC content to 212 MPa or a reduction by a factor of 7.2 for the EPI/5%PVA/20%CNC nanocomposite. The mechanical switching was in all cases complete within less than 10 min, and is likely caused by the fact that water disrupts the hydrogen-bonded reinforcing CNC network by way of acting as a competing hydrogen bond former.[20] Concomitantly, the modulus difference was much lower for the nanocomposites with 5-9% w/w CNCs (and 5% w/w PVA), where the limited mechanical reinforcement in the dry state suggests that the percolation limit has not fully been reached (*vide infra*).[17]

The water switching mechanism of the EO-EPI/PVA/CNC nanocomposites was analyzed in the context of two mechanical models. The experimental E' values of the dry nanocomposites were

compared to the theoretical prediction based on a percolation model that has frequently been employed to describe the stiffness of nanocomposites with high-aspect ratio nanofillers (**Figure 4**).[20, 45, 46] The parameters used to fit Eq. 1

$$E' = \frac{(1 - 2\emptyset + \emptyset X_r)E_s E_r + (1 - X_r)\emptyset E_r^2}{(1 - X_r)E_r + (X_r - \emptyset)E_s}, \phi = X_r \left(\frac{X_r - X_c}{1 - X_c}\right)^b \tag{1}$$

(in which X_r is the volume fraction of CNCs in the composite, X_c is volume fraction of CNCs at which the percolation threshold is reached and related to the aspect ratio A of the CNCs by $X_c =$ 0.7/A, E_r and E_s are the shear moduli of the CNCs and the EO-EPI polymer matrix, and b is the critical percolation exponent) against the experimental data include the experimentally determined CNC aspect ratio A of 11, the measured tensile storage modulus of the neat EO-EPI matrix of 2.7 MPa, and a percolation exponent b of 0.4, whereas the stiffness of the reinforcing CNC phase was used as a fit parameter (determined here to be 0.34 GPa, which corresponds well with the previously established value for this system).[42] With some deviation below (where the model neglects any reinforcement) and around the percolation threshold (ca. 6% v/v CNCs), the experimental E' values of dry EO-EPI/PVA/CNC nanocomposites fit the percolation model (pink line) quite well; at the onset of percolation, a steep increase of E' is seen and the incremental increase plateaus at the higher CNC contents investigated. The E' values of the water-swollen EO-EPI/PVA/CNC nanocomposites were compared to values calculated by the Halpin-Kardos model, which has successfully been used to describe the modulus of water-swollen CNC nanocomposites. In this case the CNC network is assumed to be disrupted by competing hydrogen bonds with water, so that the materials are better described by this mechanical model in which the filler particles are assumed to be evenly distributed the matrix without specific interactions among each other. In this analysis we considered that upon water uptake the volume fraction of CNCs is reduced and the E'

of nanocomposites were estimated base on a summation of longitudinal (E_l) and transverse (E_t) Young's moduli of nanocomposites by Eqs. 2 and 3:

$$E_l = E_m \frac{1 + \eta_l \zeta \, \varnothing_f}{1 - \eta_l \, \varnothing_f}; \quad E_t = E_m \frac{1 + 2\eta_t \zeta \, \varnothing_f}{1 - \eta_t \, \varnothing_f} \tag{2}$$

and

$$\eta_l = \frac{\dfrac{E_{lf}}{E_m} - 1}{\dfrac{E_{lf}}{E_m} + \zeta}; \quad \eta_t = \frac{\dfrac{E_{tf}}{E_m} - 1}{\dfrac{E_{tf}}{E_m} + 2} \tag{3}$$

where E_m is the modulus of the polymer matrix, $\varnothing_f$ is the volume fraction of the filler, the constant η takes into account the modulus of the matrix and CNCs, and the subscripts l and t denote the longitudinal and transverse direction of CNCs. The shape factor is defined by $\zeta = 2A$, and the longitudinal (E_{lf}) and transverse (E_{tf}) filler moduli are 105 GPa and 5 GPa, respectively.[20, 47] The fact that the model underestimates the stiffness of the water-swollen composites with high CNC content mirrors earlier findings on similar systems and reflects that the CNC network may not be fully disassembled.
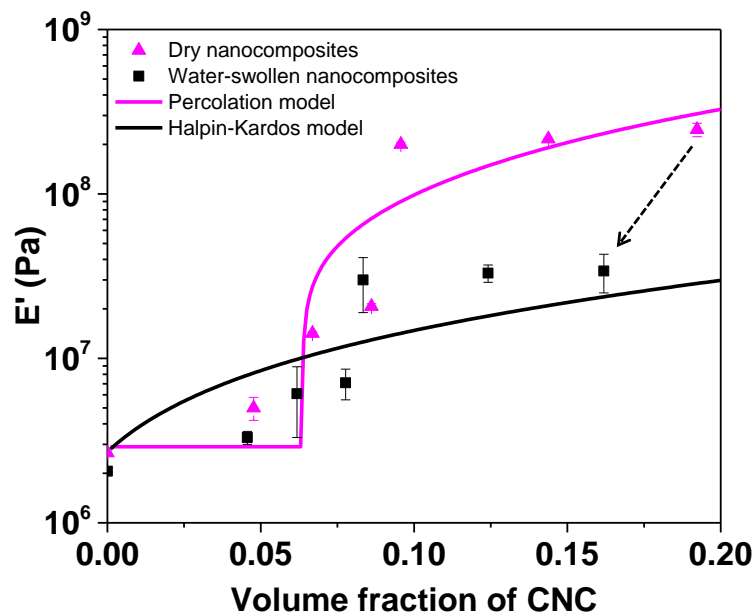
Figure 4. Experimental data (symbols) and values predicted by a percolation model or Halpin-Kardos model (lines, see text for details) of the tensile storage modulus (E') of EO-EPI/PVA/CNC nanocomposites. Shown are values for EO-EPI with 5% w/w PVA containing nanocomposites in dry state (pink line, triangles) or in wet state (black line, squares).

In summary, we have shown that the stiffness change between the dry and the water-swollen state of EO-EPI/CNC nanocomposites can be significantly enhanced by the incorporation of small amounts of PVA (1–5% w/w). The addition of PVA increases the modulus difference of EO-EPI/CNC nanocomposites via two mechanisms. On the one hand, the polymer additive increases E' of the dry nanocomposites by improving the dispersion of the CNCs in the EO-EPI matrix. In addition, the water take-up of the composites is slightly increased. We have previously shown that the addition of PVA is a versatile method to improve the dispersion and increase the stiffness of CNC nanocomposites with other polymer matrices and on that basis it appears that the framework presented here should be applicable to other CNC nanocomposites.

11

Experimental Section

Materials. EO-EPI with a co-monomer ratio of $1 : 1$ and a density of 1.39 g/cm^3 was purchased under the tradename Epichlomer from Daiso Co., Ltd., Japan. Poly(vinyl alcohol) (PVA) with a molecular weight of 85,000 – 124,000 g/mol (99% hydrolyzed), fluorescein 5(6)-isothiocyanate (FITC), dry dimethyl sulfoxide (DMSO), and sulfuric acid were purchased from Sigma-Aldrich. Solvent grade methanol was purchased from Honeywell Chemicals. All chemicals were used without further purification. CNCs, with an average length of 305 ± 80 nm, an average diameter of 27 ± 5 nm, and an average aspect ratio of 11 ± 2, were extracted from Whatman no.1 filter paper by sulfuric acid hydrolysis according to a previously reported protocol,[46] which represents a modification of the method of Dong *et al.*[48-50] The aqueous CNCs dispersion thus prepared was dried by lyophilization using a VirTis BenchTop 2K XL lyophilizer with a condenser temperature of -78 °C.

Preparation of EO-EPI/PVA/CNC and EO-EPI/CNC Nanocomposites. EO-EPI/PVA/CNC nanocomposites containing 10% w/w of CNCs and 1, 3, or 5% w/w PVA, or 5% w/w PVA and 5, 7, 9, 15, or 20% w/w CNCs, as well as a PVA-free EO-EPI/CNC reference nanocomposite with 10% w/w CNCs were prepared by solution-casting from DMSO and the materials thus obtained were compression molded into films having a thickness of 105 ± 5 μm. The procedure has been reported in detail elsewhere.[42] In order to enable a discussion of the mechanical data in the context of mechanical models, the CNC content in the nanocomposites was expressed as volume fraction (f_v) and calculated from the weight fraction (f_w) and the densities of EO-EPI ($d_m = 1.39$ g/cm^3) and CNCs ($d_f = 1.46$ g/cm^3)[46] using Eq. (4):[51]

$$f_v = \frac{f_w}{f_w + (1 - f_v)\frac{d_f}{d_m}} \tag{4}$$

Measurement of Water Uptake. The nanocomposite films were cut into rectangular shapes with a length of 30 mm and a width of 5.3 mm. The specimens were dried in vacuum at 70 °C for 24 h and then immersed in 50 mL of deionized water that was kept at ambient temperature. The samples were removed from the water bath in periodic time intervals, their surface was gently wiped dry with tissue paper, and their weight was recorded using a four-digit balance, before they were returned to the water bath. From the weight of the dry and water-swollen samples, the degree of swelling was established by Eq. 5:

$$\text{Degree of swelling (\%)} = \frac{\text{Mass of wet sample - Mass of dry sample}}{\text{Mass of dry sample}} \times 100 \qquad (5)$$

and data reported represent averages of 3 samples.

Probing Extraction of PVA from the Nanocomposites upon Immersion in Water. Nanocomposite films of EO-EPI/PVA/CNC containing 10% w/w of CNCs and 5% w/w of fluorescein-labelled PVA (PVA-F) were prepared according to a previous published procedure.[42] The dried films were cut to a weight of ca. 20 mg and immersed in 20 mL deionized water for 24 h. As a reference, 1 mg of PVA-F was dissolved separately in 20 mL deionized water by stirring the mixture at 70 °C for 24 h (thus the concentration of this solution matched the concentration expected if the extraction from the film was quantitative). The PVA-F fluorescence of the solutions was then monitored under exposure with 365 nm UV light and photographs were recorded with a Nikon D7100 digital camera equipped with a AF-S DX Zoom-NIKKOR 18-135 mm lens. Fluorescence spectra were recorded on a Horiba Fluorolog 3 spectrometer using a 450W Xenon source for excitation and a FL-1030-UP photomultiplier for fluorescence detection.

Dynamic Mechanical Analysis (DMA). The mechanical properties of the EO-EPI/PVA/CNC nanocomposite films and EO-EPI/CNC reference nanocomposite films were studied by dynamic mechanical analysis (DMA), using a TA instruments Model Q800 using a submersion setup. Rectangular films with a length of 15 mm, a width of 5.3 mm and a thickness of ca. 0.10 mm were used. The tests were conducted at ambient temperature with a strain amplitude of 15 μm and a frequency of 1 Hz. The tensile storage modulus of the nanocomposites was first measured in the dry state for 2 min. The measurement was then continued while water was added to the submersion chamber to follow the mechanical changes of the nanocomposites while immersed in water for 30 mins. The mechanical data quoted throughout the text and in Table 1 represent average values of 3 individual measurements (standard deviation is provided).

Supporting Information

Supporting Information is available from the Wiley Online Library or from the author.

Acknowledgments

Conflict of Interest

The authors declare no conflict of interest.

Keywords

References

[1]   K. Shanmuganathan, J. R. Capadona, S. J. Rowan, C. Weder, *Prog. Polym. Sci.* **2010**, *35*, 212.

[2]   L. Hsu, C. Weder, S. J. Rowan, *J. Mater. Chem.* **2011**, *21*, 2812.

[3]   D. Moatsou, C. Weder, "Chapter 12 Mechanically Adaptive Nanocomposites Inspired by Sea Cucumbers", in *Bio-inspired Polymers*, The Royal Society of Chemistry, 2017, p. 402.

[4]   L. Montero de Espinosa, W. Meesorn, D. Moatsou, C. Weder, *Chem. Rev.* **2017**, *117*, 12851.

[5]   T. Motokawa, *Comp. Biochem. Physiol., C: Comp. Pharmacol.* **1981**, *70*, 41.

[6]   T. Motokawa, *Comp. Biochem. Physiol., Part B: Comp. Biochem.* **1994**, *109*, 613.

[7]   J. Trotter, T. Koob, *J. Exp. Biol.* **1995**, *198*, 1951.

[8]   F. Thurmond, J. Trotter, *J. Exp. Biol.* **1996**, *199*, 1817.

[9]   J. A. Trotter, G. Lyons-Levy, D. Luna, T. J. Koob, D. R. Keene, M. A. L. Atkinson, *Matrix Biol.* **1996**, *15*, 99.

[10]   T. J. Koob, M. M. Koob-Emunds, J. A. Trotter, *J. Exp. Biol.* **1999**, *202*, 2291.

[11]   J. A. Trotter, G. Lyons-Levy, K. Chino, T. J. Koob, D. R. Keene, M. A. L. Atkinson, *Matrix Biol.* **1999**, *18*, 569.

[12]   G. K. Szulgit, R. E. Shadwick, *J. Exp. Biol.* **2000**, *203*, 1539.

[13]   J. P. Tipper, G. Lyons-Levy, M. A. L. Atkinson, J. A. Trotter, *Matrix Biol.* **2002**, *21*, 625.

[14]   T. Motokawa, A. Tsuchi, *Biol. Bull.* **2003**, *205*, 261.

[15]   R. Rusli, K. Shanmuganathan, S. J. Rowan, C. Weder, S. J. Eichhorn, *Biomacromolecules* **2010**, *11*, 762.

[16]   R. Rusli, K. Shanmuganathan, S. J. Rowan, C. Weder, S. J. Eichhorn, *Biomacromolecules* **2011**, *12*, 1363.

[17]   J. Mendez, P. K. Annamalai, S. J. Eichhorn, R. Rusli, S. J. Rowan, E. J. Foster, C. Weder, *Macromolecules* **2011**, *44*, 6827.

[18]   K. L. Dagnon, K. Shanmuganathan, C. Weder, S. J. Rowan, *Macromolecules* **2012**, *45*, 4707.

[19]   P. K. Annamalai, K. L. Dagnon, S. Monemian, E. J. Foster, S. J. Rowan, C. Weder, *ACS Appl. Mater. Interfaces* **2014**, *6*, 967.

[20]   J. R. Capadona, K. Shanmuganathan, D. J. Tyler, S. J. Rowan, C. Weder, *Science* **2008**, *319*, 1370.

[21]   K. Shanmuganathan, J. R. Capadona, S. J. Rowan, C. Weder, *J. Mater. Chem.* **2010**, *20*, 180.

[22]   K. Shanmuganathan, J. R. Capadona, S. J. Rowan, C. Weder, *ACS Appl. Mater. Interfaces* **2010**, *2*, 165.

[23]   A. E. Way, L. Hsu, K. Shanmuganathan, C. Weder, S. J. Rowan, *ACS Macro Lett.* **2012**, *1*, 1001.

[24]   M. Jorfi, M. N. Roberts, E. J. Foster, C. Weder, *ACS Appl. Mater. Interfaces* **2013**, *5*, 1517.

[25]   M. V. Biyani, C. Weder, E. J. Foster, *Polym. Chem.* **2014**, *5*, 5501.

[26]   M. V. Biyani, M. Jorfi, C. Weder, E. J. Foster, *Polym. Chem.* **2014**, *5*, 5716.

[27] D. A. Stone, N. D. Wanasekara, D. H. Jones, N. R. Wheeler, E. Wilusz, W. Zukas, G. E. Wnek, L. T. J. Korley, *ACS Macro Lett.* **2012**, *1*, 80.

[28] N. D. Wanasekara, D. A. Stone, G. E. Wnek, L. T. J. Korley, *Macromolecules* **2012**, *45*, 9092.

[29] M. Liu, Q. Peng, B. Luo, C. Zhou, *Eur. Polym. J.* **2015**, *68*, 190.

[30] J. R. Capadona, K. Shanmuganathan, S. Trittschuh, S. Seidel, S. J. Rowan, C. Weder, *Biomacromolecules* **2009**, *10*, 712.

[31] A. Šturcová, G. R. Davies, S. J. Eichhorn, *Biomacromolecules* **2005**, *6*, 1055.

[32] R. Rusli, S. J. Eichhorn, *Appl. Phys. Lett.* **2008**, *93*, 033111.

[33] S. Iwamoto, W. Kai, A. Isogai, T. Iwata, *Biomacromolecules* **2009**, *10*, 2571.

[34] J. Aspler, J. Bouchard, W. Hamad, R. Berry, S. Beck, F. Drolet, X. Zou, *Biopolym. Nanocompos.* **2013**.

[35] C. Endes, S. Camarero-Espinosa, S. Mueller, E. J. Foster, A. Petri-Fink, B. Rothen-Rutishauser, C. Weder, M. J. D. Clift, *J. Nanobiotechnol.* **2016**, *14*, 78.

[36] I. A. Sacui, R. C. Nieuwendaal, D. J. Burnett, S. J. Stranick, M. Jorfi, C. Weder, E. J. Foster, R. T. Olsson, J. W. Gilman, *ACS Appl. Mater. Interfaces* **2014**, *6*, 6127.

[37] M. Jonoobi, R. Oladi, Y. Davoudpour, K. Oksman, A. Dufresne, Y. Hamzeh, R. Davoodi, *Cellulose* **2015**, *22*, 935.

[38] A. Nicharat, J. Sapkota, C. Weder, E. J. Foster, *J. Appl. Polym. Sci.* **2015**, *132*.

[39] R. H. J. Otten, P. van der Schoot, *J. Chem. Phys.* **2011**, *134*, 094902.

[40] I. Balberg, C. H. Anderson, S. Alexander, N. Wagner, *Phys. Rev. B* **1984**, *30*, 3933.

[41] J. Sapkota, A. Shirole, E. J. Foster, J. C. Martinez Garcia, M. Lattuada, C. Weder, *Polymer* **2017**, *110*, 284.

[42] W. Meesorn, A. Shirole, D. Vanhecke, L. M. de Espinosa, C. Weder, *Macromolecules* **2017**, *50*, 2364.

[43] A. Mercanzini, K. Cheung, D. Buhl, M. Boers, A. Maillard, P. Colin, J. C. Bensadoun, A. Bertsch, A. Carleton, P. Renaud, "Demonstration of cortical recording and reduced inflammatory response using flexible polymer neural probes", in *2007 IEEE 20th International Conference on Micro Electro Mechanical Systems (MEMS)*, 2007573.

[44] J. P. Harris, A. E. Hess, S. J. Rowan, C. Weder, C. A. Zorman, D. J. Tyler, J. R. Capadona, *J. Neural Eng.* **2011**, *8*, 046010.

[45]   V. Favier, H. Chanzy, J. Y. Cavaille, *Macromolecules* **1995**, *28*, 6365.

[46]   J. Sapkota, S. Kumar, C. Weder, E. J. Foster, *Macromol. Mater. Eng.* **2015**, *300*, 562.

[47]   J. J. Fallon, B. Q. Kolb, C. J. Herwig, E. J. Foster, M. J. Bortner, *J. Appl. Polym. Sci.* **2019**, *136*, 46992.

[48]   X. M. Dong, T. Kimura, J.-F. Revol, D. G. Gray, *Langmuir* **1996**, *12*, 2076.

[49]   X. M. Dong, D. G. Gray, *Langmuir* **1997**, *13*, 2404.

[50]   X. M. Dong, J.-F. Revol, D. G. Gray, *Cellulose* **1998**, *5*, 19.

[51]   P. D. Bradford, X. Wang, H. Zhao, J.-P. Maria, Q. Jia, Y. T. Zhu, *Compos. Sci. Technol.* **2010**, *70*, 1980.
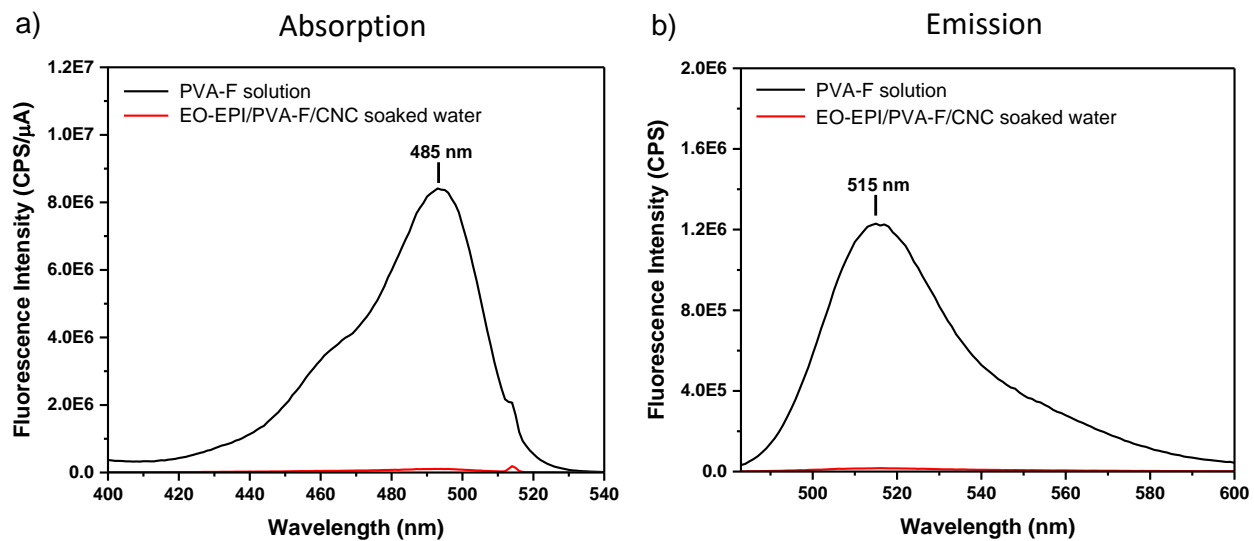
Supporting Information

a)
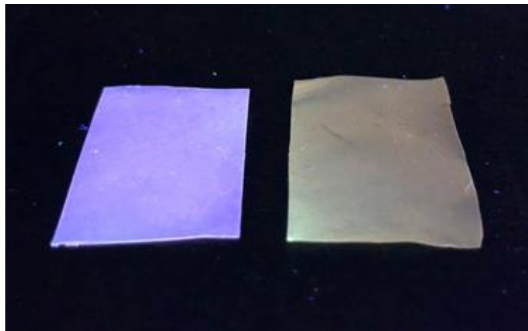
b)

Figure S1. a) Picture of EO-EPI/10% w/w CNC film (left) and EO-EPI/PVA-F/CNC nanocomposite film containing 10% w/w CNCs and 5% w/w PVA-F (right). b) Picture of 50 μg/mL PVA-F solution (left) and nanocomposite film of EO-EPI/PVA-F/CNC soaked in water (right).

Figure S2. Fluorescence absorption (a) and emission (b) spectra of 50 μg/mL PVA-F solution and water in which the EO-EPI/PVA-F/CNC nanocomposite film had been immersed for 24 h.